Journal of Applied Informatics and Computing (JAIC)
Vol.10, No.3, June 2026, pp. 2502~2511
e-ISSN: 2548-6861

A Robust Voting Ensemble Framework for Predicting Thermal Stability in Zn-Based Metal–Organic Frameworks

Taufiqul Umam[1] , Harun Al Azies[1,2] , Muhamad Akrom[1,2] , Ananta Surya Pratama[1] , Muhammad Diva Irnanda[1]
[1]Study Program in Informatics Engineering, Faculty of Computer Science, Universitas Dian Nuswantoro
[2] Research Center for Quantum Computing and Materials Informatics, Faculty of Computer Science, Universitas Dian Nuswantoro
111202315273@mhs.dinus.ac.id [1] , harun.alazies@dsn.dinus.ac.id[2] , m.akrom@dsn.dinus.ac.id [3] , 111202315107@mhs.dinus.ac.id [4] , 111202315484@mhs.dinus.ac.id [5]

Article Info

Article history:

Received 2026-04-11
Revised 2026-05-08
Accepted 2026-05-25

Keyword:

Metal Organic Frameworks,
Robust Regression,
Thermal Stability,
Voting Ensemble,
Zinc-Based MOFs.

ABSTRACT

The prediction of thermal stability (TS) in zinc-based metal–organic frameworks (Zn-MOFs) is often challenged by experimental cost and distributional heterogeneity in materials datasets. This study proposes a median-based robust voting ensemble to model the TS of 151 Zn-MOF samples using four structural descriptors, nN, nZn, Het, and Lig. The framework integrates five robust linear estimators and is benchmarked against a linear kernel Support Vector Regression (SVR) model to evaluate predictive stability and generalization performance. The proposed ensemble demonstrates superior test performance (R^2 = 0.9986; RMSE = 0.0023) compared to SVR (R^2 = 0.9492; RMSE = 0.0213), indicating enhanced robustness under heterogeneous data conditions. Feature importance analysis identifies nitrogen coordination density and heteroatomic environment as the dominant contributors to TS prediction, while zinc center quantity and ligand topology exhibit comparatively minor influence. These findings confirm that median-based robust aggregation improves predictive reliability and provides chemically interpretable insight, offering a data-driven approach for the rational design and screening of thermally stable Zn-MOF materials.

I. INTRODUCTION

Global dependence on fossil fuels remains the primary driver of anthropogenic carbon dioxide (CO_2) emissions and climate change. The Global Carbon Budget 2022 reports that CO_2 emissions from fossil fuel combustion and industrial processes reached approximately 36–37 $GtCO_2$ per year, with the energy sector accounting for the largest share of total anthropogenic emissions [1]. Recent updates further indicate that global emissions have not yet demonstrated a sustained structural decline despite the expansion of renewable energy capacity [2]. Beyond environmental impacts, fossil-based energy systems are associated with price volatility, supply insecurity, and geopolitical risks that affect macroeconomic stability [3]. These findings underscore that the transition toward low-carbon energy systems is not solely an environmental objective but also a systemic economic necessity. Renewable energy technologies, energy storage systems, and hydrogen-based solutions have been identified as central pillars of energy system decarbonization[4], [5]. However, the effectiveness of clean energy technologies depends fundamentally on the performance and durability of the underlying functional materials. Parameters such as thermal stability, chemical stability, conductivity, and cycling durability directly determine operational efficiency and service[6], [7]. Consequently, material limitations represent a critical bottleneck in the large-scale deployment of sustainable energy technologies.

Metal Organic Frameworks (MOFs) constitute a class of crystalline porous materials composed of metal nodes coordinated with organic ligands. Their modular architecture enables precise control over surface area, pore size, and chemical functionality [8]. Among various MOF derivatives, Zn-based MOFs (Zn-MOFs) have attracted particular attention due to the coordination characteristics of Zn^{2+} ions, which facilitate the formation of lightweight and highly

porous frameworks [9], [10]. These structural attributes are advantageous for applications in gas storage, catalysis, and electrochemical energy systems. Nevertheless, thermal stability remains a critical challenge. Elevated operating temperatures may induce ligand decomposition, phase transformation, and structural collapse, leading to significant degradation in functional performance [11], [12]. Thermal stability is commonly evaluated using Thermogravimetric Analysis (TGA), which measures mass changes as a function of temperature under controlled conditions. Although TGA provides reliable measurements, it requires carefully controlled experiments, repeated trials, and substantial laboratory resources [13]. When applied to large-scale material screening, this experimental approach becomes time-intensive and economically inefficient. Therefore, predictive methodologies capable of estimating thermal stability in a rapid and reliable manner are increasingly required.

Recent advances in machine learning (ML) have introduced data-driven paradigms for accelerating materials discovery and property prediction [14], [15]. ML models have been successfully employed to predict various MOF properties, including gas adsorption capacity, surface area, and chemical stability [16], [17]. However, materials datasets are frequently heterogeneous and often contain noise and outliers arising from variations in synthesis procedures, experimental conditions, and structural diversity [18]. Exploratory data analysis conducted in this study reveals the presence of significant outliers across several descriptor variables. Such distributional characteristics may adversely affect parameter estimation in conventional linear regression models, which are inherently sensitive to extreme residuals.

Recent studies have examined machine-learning-based quantitative structure–property relationships (QSPR) for predicting the thermal stability of Zn-MOF systems. Moharramnejad et al. (2022) developed a multilinear regression model using structural descriptors, including nitrogen content, zinc atoms, and heteroatomic interactions, reporting coefficients of determination of 0.999 for both the training and test sets. Subsequently, Trisnapradika and Akrom (2024) evaluated ridge and kernel ridge regression on the same dataset, demonstrating that regularized linear methods can maintain high predictive accuracy while reducing multicollinearity [19]. Beyond classical and regularized regression, robust modeling strategies have also been introduced. Harun Al Azies et al. (2024) proposed a robust regression (RR) framework to mitigate the influence of outliers on the prediction of Zn-MOF thermal stability. The study demonstrated that robust regression outperformed traditional multiple linear regression and successfully predicted the TS of a novel Zn-MOF compound with experimental validation, confirming the importance of handling data contamination in materials informatics modeling [20]. These studies confirm the feasibility of linear, regularized, and robust regression approaches for Zn-MOF TS prediction. However, despite the demonstrated advantages of robust regression, prior work has primarily relied on single-model estimation frameworks. The potential benefit of aggregating multiple robust estimators through ensemble strategies to further constrain the influence of extreme observations and reduce inter-estimator variability has not been systematically explored.

To address this limitation, the present study proposes a robust ensemble regression framework based on median voting. The proposed approach integrates five robust linear regression estimators, such as Theil–Sen, M-estimator, RANSAC, S-estimator, and Least Trimmed Squares, each sharing the same linear functional form while employing distinct parameter estimation mechanisms to reduce sensitivity to extreme observations and contaminated residuals. These estimators are aggregated using a median voting scheme to enhance predictive stability. For comparative analysis, Support Vector Regression (SVR) with a linear kernel is employed as a representative margin-based linear regression model without explicit robustness mechanisms. This study evaluates the effectiveness of the proposed median-based robust ensemble in predicting the thermal stability of Zn-MOFs under heterogeneous descriptor conditions, analyzes the contribution of structural and chemical descriptors through model-based interpretation, and systematically compares its predictive performance and generalization stability against linear-kernel SVR to determine whether robust estimator aggregation provides statistically and practically significant improvements over a single margin-based linear model. By integrating robustness-oriented modeling within a material informatics framework, this research seeks to establish a methodologically rigorous, empirically grounded approach to improve predictive Reliability in thermally sensitive Zn-MOF systems.

II. METHOD

This study employed a structured machine learning workflow consisting of data preparation, exploratory analysis, preprocessing, model development, cross-validation-based performance comparison, statistical testing, and independent test evaluation. The methodological design was constructed to ensure robustness against descriptor redundancy and potential data contamination. The overall research workflow is presented in Figure 1.

A. Data Collection

The dataset used in this study was obtained from the work of [21], who developed a quantitative structure–property relationship (QSPR) model to predict the thermal stability of Zn-based metal–organic frameworks (Zn-MOFs). The dataset consists of 151 Zn-MOF compounds characterized by experimentally measured thermal stability values derived from thermogravimetric analysis (TGA). In the original study, thermal stability (TS) is defined as the temperature corresponding to the onset of the first significant mass loss observed in the TGA curve, indicating the initiation

of structural decomposition of the framework. This value, commonly referred to as (T_{onset}), is expressed in degrees

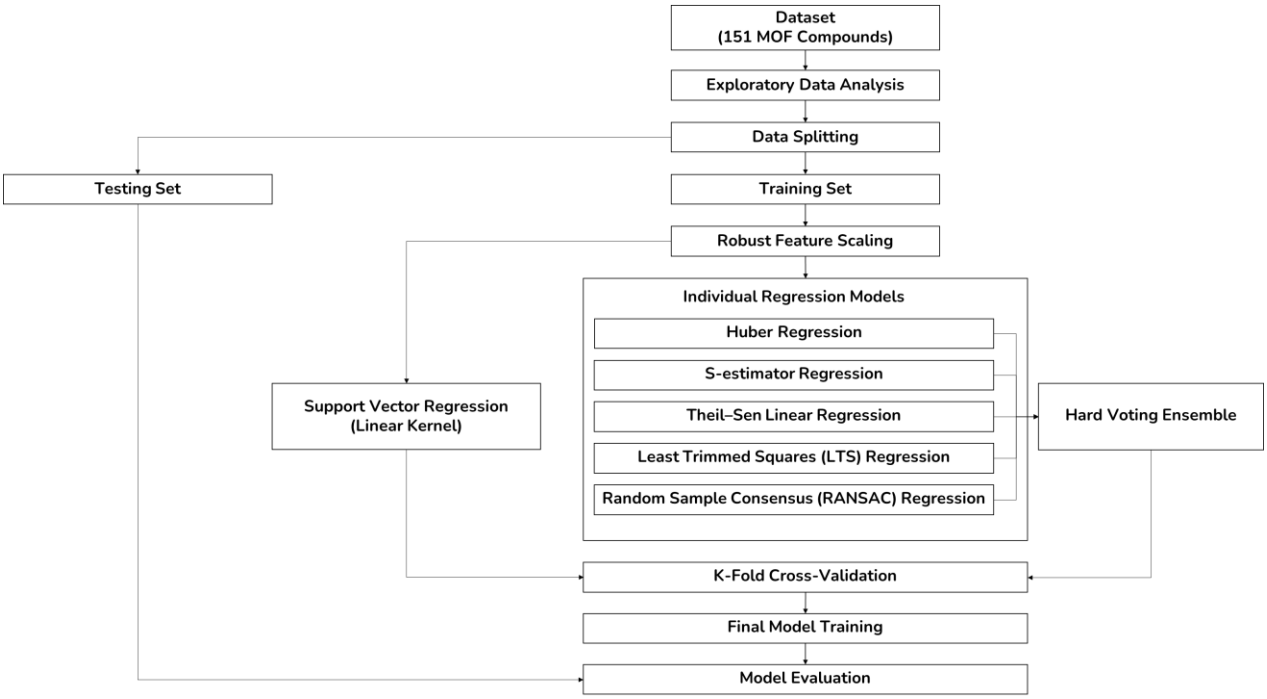

Figure 1. Proposed Robust Ensemble Regression Framework for Predicting Zn-MOF Thermal Stability

Celsius (°C) and reflects the thermal resistance of the material under controlled heating conditions.

Following the formulation adopted in the original dataset, the target variable in this study is defined as log(TS), representing the base-10 logarithm of TS. The transformation is expressed as ($\log(TS) = \log_{10}(T_{onset})$). This logarithmic transformation converts the response into a dimensionless variable, reduces scale sensitivity, and improves numerical stability, thereby facilitating more reliable modeling of the structure–property relationship. Each compound is represented by four structural descriptors:

1. The descriptor nN denotes the number of nitrogen donor atoms coordinating to the Zn^{2+} center and can be interpreted as a coordination number component that influences ligand field strength and metal–ligand bond stability, as widely discussed in coordination chemistry studies [22], [23]. Mathematically, nN is a discrete count variable that contributes linearly to the regression model and reflects the density of strong donor interactions within the framework.
2. The nZn, represents the number of zinc atoms within the secondary building unit (SBU), serving as a proxy for metal cluster size and connectivity. The role of SBUs in defining MOF topology and stability has been extensively[10], [22]. From a modeling perspective, nZn acts as a structural scaling variable that captures variations in coordination network complexity.
3. Het, a numerical descriptor representing quantifies heteroatomic interactions between the organic linker and the metal center. Chemically, it reflects electronic effects such as ligand–metal orbital overlap, charge transfer, and ligand field interactions, which are known to influence bond strength and thermal resistance, as highlighted[11], [24]. In the QSPR formulation, Het is treated as a continuous numerical variable derived from electronic interaction considerations, enabling the model to capture variations in coordination environment beyond simple atom counts.
4. Lig, a numerical descriptor reflecting the contribution of molecular fragments within the organic linker. This variable encodes structural complexity and connectivity patterns, which play a role in determining framework stability and degradation behavior[11], [12]. From a mathematical standpoint, Lig functions as a continuous descriptor that complements coordination-based variables by incorporating ligand-specific structural information. Together, these descriptors provide a compact yet chemically meaningful representation of Zn-MOF structures for predictive modeling.

B. Data Preprocessing

The data preprocessing stage involved train–test splitting and feature scaling. The dataset was partitioned into a training set (80%) and a test set (20%) to enable independent performance evaluation on unseen data and to provide an

unbiased estimate of the model's generalization capability [25]. Feature scaling was applied using the Robust Scaler, which performs a transformation based on the median and interquartile range (IQR) [26]. The scaler was fitted exclusively to the training set and subsequently applied to both the training and test data to prevent data leakage [26]. This approach was adopted in response to the distributional characteristics identified during exploratory analysis, including asymmetry and extreme observations. Compared to mean-based normalization methods, robust scaling reduces sensitivity to outliers while preserving the relative structure of the data [26].

C. Exploratory Data Analysis

Exploratory Data Analysis was conducted to examine the statistical characteristics of the Zn-MOF dataset before model development. The analysis began with the computation of skewness values for each predictor variable (nN, nZn, Het, and Lig) and the response variable log(TS) to assess distributional asymmetry [27]. The results indicate that several variables exhibit non-zero skewness, suggesting deviations from perfectly symmetric distributions. Boxplots were then used to evaluate central Tendency, dispersion, and the presence of extreme observations [28]. The plots reveal several data points outside the interquartile range, indicating potential outliers in the dataset. Such distributional patterns are consistent with structurally diverse materials data and may Influence parameter estimation in conventional regression models. Pearson correlation analysis was subsequently performed to examine linear relationships between predictors and log(TS) and to assess potential multicollinearity among descriptors [29]. The correlation structure provides preliminary insight into the contribution of structural variables to thermal stability.

D. Model Development

Model development was designed to address the distributional heterogeneity and presence of outliers identified in the Zn-MOF dataset. Conventional ordinary least squares regression relies on quadratic loss and is therefore sensitive to extreme residuals [30]. To enhance parameter stability under partial contamination, a robust linear regression framework was adopted. Five robust linear estimators were implemented as base learners. Theil–Sen regression estimates regression coefficients using median-based slope calculations, providing robustness against extreme observations [31]. The Huber M-estimator applies a piecewise loss function that combines squared and absolute error, reducing the influence of large residuals while retaining efficiency for small errors [30]. RANSAC regression iteratively fits models to random subsets of inliers, excluding observations that deviate substantially from the consensus pattern [32]. The S-estimator minimizes a robust measure of residual scale, achieving a high breakdown point under contamination [33]. Least Trimmed Squares (LTS) regression estimates parameters by minimizing the sum of the smallest squared residuals, effectively trimming extreme observations [34]. Hyperparameter tuning for each estimator was performed using a 10-fold cross-validation grid search on the training set [35].

The optimized base learners were then aggregated using a median-based hard voting ensemble For a given input (x), the final prediction is defined as:

$$\hat{y}_{ensemble}(x) = median_{i\in\{1,\dots,k\}}\ \hat{y}_i(x) \qquad (1)$$

where $(\hat{y}i(x))$ *denotes the prediction of the (i)-th base estimator and* $(\hat{y}(j)(x))$ represents the $(j)-th$ order statistic obtained by sorting the predictions in ascending order. The median corresponds to the central value of the ordered prediction set, providing a robust estimator of central tendency that is less sensitive to extreme values compared to mean-based aggregation.

Model generalization was assessed using 10-fold cross-validation applied exclusively to the training data. For benchmarking purposes, Support Vector Regression (SVR) with a linear kernel was implemented to ensure structural comparability with the linear robust estimators while representing a margin-based regression framework [36]. The SVR model was configured with the following parameters: linear kernel, cost parameter $C = 50$, epsilon-insensitive loss parameter $\varepsilon = 0.01$, and gamma set to "scale". Hyperparameter tuning was also performed using grid search cross-validation on the training data to ensure fair comparison. The SVR model was configured with the following parameters: linear kernel, cost parameter $C = 50$, epsilon-insensitive loss parameter $\varepsilon = 0.01$, and gamma set to "scale". Hyperparameter tuning was also performed using grid search cross-validation on the training data to ensure fair comparison.

E. Model Evaluation

The predictive performance of the regression models in estimating the thermal stability (log TS) of Zn-MOF materials was evaluated using three primary metrics, the coefficient of determination (R^2), Mean Absolute Error (MAE), and Root Mean Square Error (RMSE). These metrics are widely adopted in regression analysis because they provide complementary information regarding model explanatory power and prediction error magnitude [37]. The coefficient of determination (R^2) quantifies the proportion of variance in the target variable that is explained by the model relative to the total variance of the observed data. It is mathematically defined as:

$$R^2 = 1 - \frac{\sum_{i=1}^{n}(y_i - \hat{y}_i)^2}{\sum_{i=1}^{n}(y_i - \bar{y})^2} \qquad (1)$$

where $y_i$denotes the actual value, $\hat{y}_i$represents the predicted value, $\bar{y}$is the mean of the observed values, and $n$is the number of samples. A higher R^2 value indicates greater explanatory capability of the model. Mean Absolute Error

(MAE) measures the average absolute difference between actual and predicted values and is defined as:

$$MAE = \frac{1}{n}\sum_{i=1}^{n}|y_i - \hat{y}_i| \quad (2)$$

MAE expresses prediction error in the same unit as the target variable and treats all deviations linearly, making it less sensitive to extreme errors. Root Mean Square Error (RMSE) is defined as the square root of the mean of squared residuals.

$$RMSE = \sqrt{\frac{1}{n}\sum_{i=1}^{n}(y_i - \hat{y}_i)^2} \quad (3)$$

RMSE penalizes larger deviations more heavily due to the squaring of residuals prior to averaging. Consequently, RMSE is particularly effective in detecting substantial prediction errors and evaluating model performance under scenarios where large deviations are undesirable. Performance metrics were computed using 10-fold cross-validation on the training set to obtain stable performance estimates. Final evaluation was conducted on the independent test set to assess generalization capability. To examine whether performance differences between the robust voting ensemble and linear-kernel Support Vector Regression (SVR) were statistically significant, the Wilcoxon signed-rank test was applied to the cross-validation results [38]. This non-parametric test was selected because it does not assume normal distribution of paired differences and is appropriate for comparing model performance across folds.

III. RESULTS AND DISCUSSION

A. *Exploratory Analysis and Problem Characterization*

An exploratory analysis was conducted to characterize the statistical structure of the Zn-MOF dataset and identify potential modeling constraints. Because the response variable log(TS) lies within a relatively narrow range, understanding the dispersion, asymmetry, and inter-feature relationships of the descriptors is critical for determining whether conventional linear regression assumptions are appropriate.

TABLE 1.
STATISTIC DESCRIPTION OF ZN-MOF DATASET

Variable	Count	Mean	Std	Min	25%
nN	151	6.0876	7.6040	0.0000	2.0000
nZn	151	3.3532	8.1006	1.0000	1.0000
Het	151	-4.1499	10.3363	-55.8750	-4.9790
Lig	151	2.4873	1.3879	-0.8100	1.5510
TS	151	2.5744	0.0904	2.2040	2.5440

Table X presents the descriptive statistics of the Zn-MOF dataset consisting of 151 samples with four structural descriptors (nN, nZn, Het, and Lig) and the target variable log(TS). The results indicate substantial variability in the descriptor space, particularly for nZn and Het, which exhibit wide ranges and extreme values, reflecting heterogeneous structural characteristics across samples. In contrast, log(TS) shows a relatively narrow distribution with low standard deviation, suggesting that thermal stability varies within a limited range despite the diversity of input features. This imbalance between feature variability and target dispersion highlights the importance of further examining distributional properties, particularly skewness, to better understand asymmetry and the presence of extreme observations that may affect model performance.

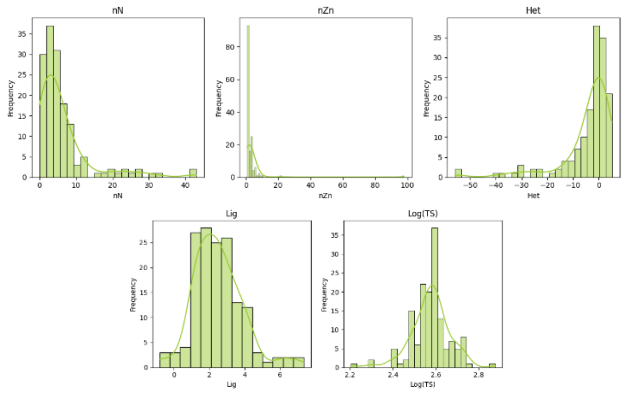

Figure 2. Distribution and Skewness Analysis of Zn-MOF Variables

Figure 2 presents the distributions of nN, nZn, Het, Lig, and log(TS) using histograms combined with kernel density estimation. The structural descriptors display heterogeneous distributional patterns. Both nN and nZn exhibit clear positive skewness, with a concentration of observations at lower values and extended upper tails. In particular, nZn includes extreme observations approaching 100, indicating the presence of structurally atypical frameworks. The descriptor Het shows negative skewness, extending to approximately −50, reflecting asymmetric heteroatom interactions across coordination environments. In contrast, Lig and log(TS) appear comparatively more symmetric. However, log(TS) is confined within a narrow interval around 2.5–2.6, indicating limited variation in thermal stability relative to structural variability.

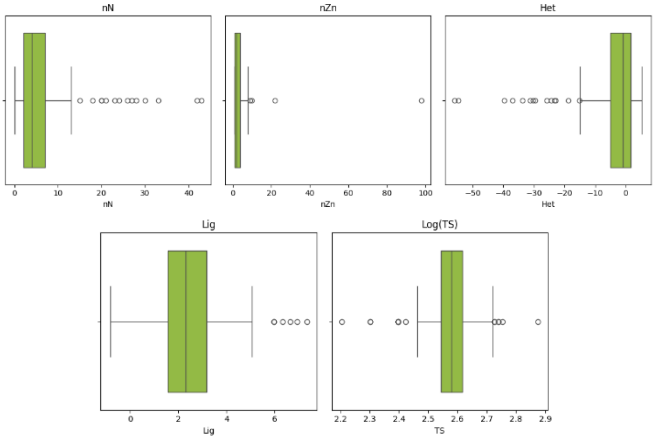

Figure 3. Boxplot Visualization of Zn-MOF Variables

The dispersion patterns observed in the histograms are further confirmed in Figure 3 through boxplot analysis. Several variables contain observations beyond the 1.5×IQR threshold, indicating the presence of extreme values. The most pronounced upper-tail outliers occur in nZn, while nN also shows multiple high-leverage points. It exhibits a substantially lower tail, consistent with its negative skewness. Even variables with tighter interquartile ranges, such as Lig and log(TS), contain isolated observations outside whisker boundaries. In regression models based on quadratic loss minimization, such extreme points can disproportionately Influence parameter estimation, potentially reducing model stability.

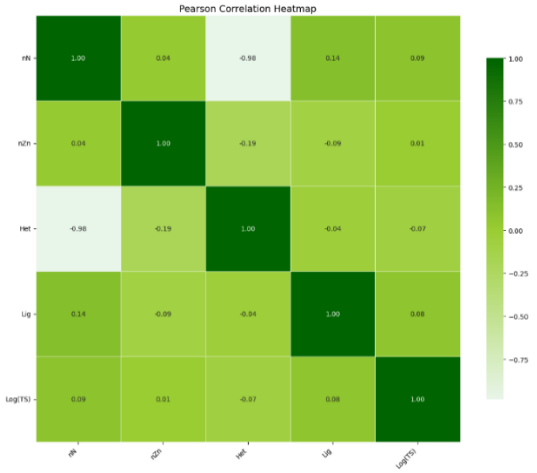

Figure 4. Pearson Correlation Matrix of Structural Descriptors and log(TS)

The correlation structure provides additional insight into the statistical relationships among descriptors and thermal stability. As shown in Figure 4, the Pearson correlation analysis reveals a near-perfect negative correlation (−0.98) between nN and Het, indicating a substantial linear relationship between these two descriptors. This suggests that nitrogen content and heteroatomic interaction parameters encode overlapping structural information within Zn-MOF coordination environments. Such strong multicollinearity may reduce coefficient stability in conventional linear regression models.

TABLE 2.
STATISTICAL SIGNIFICANCE OF DESCRIPTOR–LOG(TS) CORRELATIONS

Descriptor	Pearson Correlation (r)	p-value
nN	0.089	0.272
Lig	0.083	0.308
Het	-0.071	0.387
nZn	0.014	0.861

In contrast, the correlations between individual descriptors and log(TS) remain weak. As presented in Table 1, Pearson correlation coefficients range from −0.0709 to 0.0899, and all corresponding p-values exceed 0.05. These results indicate that none of the structural descriptors shows a statistically significant linear association with log(TS) when evaluated independently. The absence of significant univariate relationships suggests that a single structural variable does not drive thermal stability in Zn-MOF systems. However, rather than combined multivariate effects, it is more likely governed by it. The absence of statistically significant univariate correlations suggests that no single structural descriptor governs thermal stability in Zn-MOF systems. Instead, the relationship appears multivariate and potentially nonlinear. The coexistence of strong inter-descriptor correlation and weak feature–target association highlights structural redundancy alongside limited individual explanatory power. This statistical pattern may challenge parameter stability in ordinary least-squares regression and provides empirical justification for employing robust estimators and ensemble aggregation to enhance predictive reliability.

B. Robust Ensemble Performance in Zn-MOF Thermal Stability Prediction

Following the distributional analysis, the predictive performance of the linear-kernel Support Vector Regression (SVR) and the median-based robust voting ensemble was evaluated using repeated resampling and independent testing to assess stability and generalization capability. The cross-validation results are presented in Figure 5.

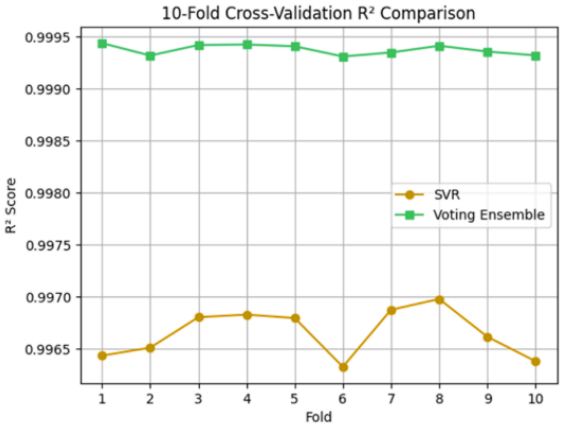

Figure 5. Cross-Validation Performance of Robust Ensemble and SVR in Zn-MOF Thermal Stability Prediction

Figure 5 presents the results of 10-fold cross-validation applied to both models. Across all folds, the robust voting ensemble consistently achieved higher R^2 values than SVR. The SVR model yielded R^2 scores ranging from 0.996327 to 0.996979, whereas the voting ensemble produced values between 0.999310 and 0.999438. In addition to higher average performance, the ensemble showed lower fold-to-fold dispersion, indicating greater stability across repeated data partitions. The consistent performance gap of approximately 0.002–0.003 R^2 per fold suggests that robust aggregation improves predictive consistency in the presence of structural heterogeneity.

TABLE 3.
WILCOXON SIGNED-RANK TEST FOR MODEL PERFORMANCE IN ZN-MOF THERMAL STABILITY PREDICTION

Test Statistic (W)	P-value
0.0	0.002*

Note: *) Significant at $\alpha = 0.05$. Since $p < \alpha$, the null hypothesis of no median difference is rejected.

To determine whether the observed performance difference was statistically significant, a Wilcoxon signed-rank test was applied to the paired cross-validation R^2 values. The results are summarized in Table 2. The test yielded a statistic of 0.0 and a p-value of 0.001953125, which is below the 0.05 threshold. This indicates a statistically significant difference in performance between the two models across folds.

TABLE 4.
COMPARATIVE TRAINING AND TESTING PERFORMANCE IN ZN-MOF THERMAL STABILITY PREDICTION

Metric	Mode	Voting Ensemble	SVR	Random Forest
RMSE	Train	0.00219	0.00496	0.07162
	Test	0.00232	0.02125	0.09121
MAE	Train	0.00181	0.00407	0.05309
	Test	0.00193	0.00758	0.06463
R^2	Train	0.99938	0.99681	0.33685
	Test	0.99861	0.94923	0.65072

Note: The Voting Ensemble achieved the best performance across all evaluation metrics on the test set.

While cross-validation assesses model stability, independent test evaluation provides additional insight into generalization capability. Table 4 compares the training and testing performance of the proposed Voting Ensemble model against SVR and Random Forest. Among the evaluated models, the Voting Ensemble consistently achieved the best performance across all evaluation metrics. The model maintained highly consistent results between training and testing, with R^2 values of 0.99938 and 0.99861, respectively. In addition, the corresponding RMSE and MAE values remained very low on the test set (RMSE = 0.00232; MAE = 0.00193), indicating minimal performance degradation when applied to unseen data. This consistency suggests that the proposed ensemble successfully captures the underlying relationship between structural descriptors and thermal stability without exhibiting substantial overfitting.

The linear SVR model also demonstrated strong predictive capability, although a noticeable decline was observed from training to testing performance. The testing R^2 decreased to 0.94923, accompanied by increased RMSE and MAE values, indicating higher sensitivity to distributional variation within the Zn-MOF dataset. In contrast, Random Forest produced substantially lower performance, with testing R^2 reaching only 0.65072 and relatively large prediction errors. This behavior suggests that the descriptor–target relationship in the Zn-MOF dataset is more effectively captured by the proposed robust linear ensemble framework than by the tree-based ensemble approach. Overall, the results indicate that combining multiple robust linear estimators through median-based aggregation provides superior predictive stability and generalization performance for Zn-MOF thermal stability prediction.

Figure 6 presents complementary visual comparisons of prediction behavior for both models. The upper panels display scatter plots of observed versus predicted log(TS), while the lower panels illustrate sample-wise prediction trajectories. In panel (a), corresponding to the SVR scatter plot, several points deviate from the 1:1 reference line, particularly within the intermediate log(TS) range. This dispersion indicates uneven residual distribution and localized prediction instability. In contrast, panel (b) shows the voting ensemble scatter plot, where predictions cluster more tightly along the diagonal, suggesting reduced residual variance and improved global alignment. Panels (c) and (d) provide sample-index comparisons between actual and predicted values. In panel (c), the SVR model exhibits noticeable deviations at specific sample indices, especially around regions with abrupt log(TS) fluctuations.

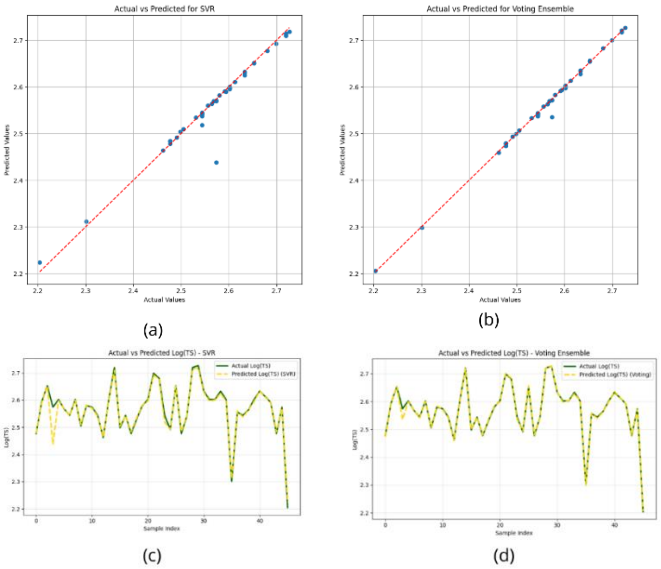

Figure 6. Observed versus Predicted log(TS) for Zn-MOF Thermal Stability Models: (a) SVR Scatter, (b) Voting Scatter, (c) SVR Trajectory, (d) Voting Trajectory

These localized mismatches reflect reduced stability in capturing structural variability. Conversely, panel (d) demonstrates that the voting ensemble closely follows the actual trajectory across nearly all samples, including regions with higher variation. The tighter overlap between predicted and actual curves indicates improved local consistency and smoother residual behavior. Both visual analyses consistently show that the robust voting ensemble achieves superior generalization performance compared to linear-kernel SVR.

C. Model Interpretation and Structural Insight

In addition to predictive performance, permutation feature importance was analyzed to identify the structural descriptors

most influential in determining log(TS) in Zn-MOF systems. The relative contributions of the four descriptors are presented in Figure 7.

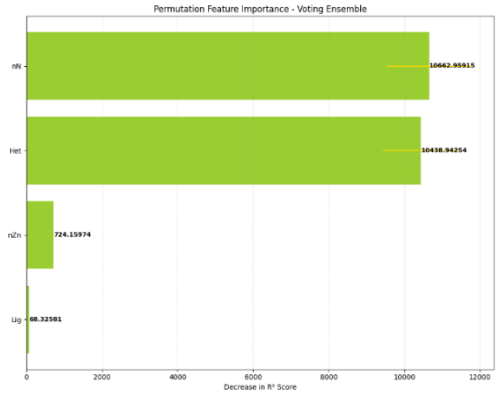

Figure 7. Permutation Feature Importance for log(TS) Prediction in Zn-MOF Systems

1) Contribution of Nitrogen Coordination Density to log(TS)

The descriptor nN exhibits the highest permutation importance (10,664.31), indicating that perturbation of nitrogen donor counts produces the largest degradation in predictive accuracy. This finding is chemically consistent with the coordination geometry reported in Zn-MOF systems. In the Zn-MOF synthesized by Shao et al., Zn(II) adopts a ZnN_4O_2 octahedral coordination environment with Zn–N bond lengths ranging from 2.24–2.29 Å. These Zn–N interactions directly govern the framework's structural stability[23]. Moreover, in the tri-metallic MOF-COF heterostructure study, Zn–N bonds were shown to resist dissociation under thermal stress, contributing to enhanced thermal endurance up to 817.6 K. The authors explicitly attribute superior thermal stability to robust metal–ligand coordination [24]. Therefore, the high importance of nN in the present model aligns with experimental and computational evidence that nitrogen coordination density strengthens metal–ligand bonding and delays thermally induced framework collapse.

2) Influence of Heteroatomic Environment on log(TS)

The descriptor Het shows a similarly high importance score (10,440.27), reinforcing the critical role of heteroatomic composition in thermal behavior. The Zn-MOF structural analysis by Shao et al. demonstrates that ligand design directly modulates coordination topology and electronic environment. Heteroatoms influence ligand–ligand charge transfer (LLCT) and ligand–metal interactions, both of which affect bond strength and stability (Shao et al., 2021). Additionally, the MOF-COF heterostructure study shows that altering the metal node from Cu to Zn significantly alters the thermomechanical response. This confirms that the electronic structure around coordination centers governs thermal endurance. In the context of Zn-MOFs, heteroatomic variations are likely to alter electron-donating capacity, ligand-field effects, and bond polarity. This directly impacts bond dissociation resistance at elevated temperature(Ding et al., 2025). The near-perfect negative correlation previously observed between nN and Het suggests overlapping structural encoding, yet both remain dominant contributors to log(TS).

3). Influence of Zinc number on log(TS)

The importance score for nZn (724.25) is substantially lower. Although Zn–ligand coordination is fundamental, the literature suggests that stability depends more on bond quality than metal quantity. In the MOF-COF system, thermal degradation occurred when coordination bonds ruptured under high temperature (Shao et al., 2021). This indicates that coordination integrity, not metal count alone, determines thermal endurance. Thus, increasing the number of Zn centers without strengthening the coordination environment does not proportionally enhance stability (Ding et al., 2025). The model's reduced sensitivity to nZn is therefore chemically plausible.

4) Limited Effect of on log(TS)

The Lig descriptor has the smallest importance score (68.33), indicating limited independent explanatory power. In the Zn-MOF structure reported by Shao et al., the framework topology is determined by ligand connectivity and coordination pattern (Shao et al., 2021). However, thermal decomposition in MOF systems typically initiates through metal–ligand bond rupture rather than ligand backbone collapse. The thermomechanical simulations in the heterostructure study further show that bond dissociation at coordination nodes marks the onset of structural failure (Ding et al., 2025). This supports the observation that ligand topology alone contributes less to TS prediction than coordination-chemistry descriptors.

5) SHapley Additive exPlanations (SHAP) Analysis

Figure 8. SHAP Analysis from prediction of Log(TS)

To complement the feature importance analysis, SHAP force visualization was further examined to illustrate how individual descriptors contribute to a specific prediction. As shown in Figure X, the predicted log(TS) value is primarily influenced by the interaction between nN and Het, which is consistent with the global SHAP importance ranking discussed previously. In this example, the contribution of nN shifts the prediction toward a higher thermal stability region, indicating that the presence of nitrogen donor atoms strengthens the coordination interaction between the organic linker and the Zn^{2+} center. This behavior is chemically reasonable because nitrogen-containing ligands generally enhance coordination strength and improve framework rigidity.

The Het descriptor also contributes positively to the prediction, reflecting the role of heteroatomic electronic interactions in stabilizing the metal–ligand environment through orbital overlap and charge distribution effects. In contrast, the contributions of nZn and Lig are comparatively smaller, suggesting that although framework topology and ligand fragment composition still influence the prediction, their effects are less dominant for this particular Zn-MOF structure. Overall, the local SHAP interpretation supports the earlier feature importance findings and demonstrates that the proposed model captures chemically meaningful relationships between coordination structure, electronic interaction, and thermal stability behavior in Zn-MOF materials.

D. The Rational design and screening

To demonstrate the applicability of the proposed model for rational material design and screening, a prediction experiment was conducted on the $Zn_3(DDB)(DPE)\cdot H_2O$ framework using the Robust Voting Ensemble model. Table 3 presents the structural descriptor values together with the corresponding experimental and predicted log(TS) values. The close agreement between the experimental result and model prediction indicates that the proposed framework is capable of capturing the underlying relationship between coordination environment, ligand characteristics, and thermal stability behavior in Zn-MOF structures.

TABLE 3.
LOG(TS) PREDICTION VALUE OF ZN3(DDB)(DPE)·H2O BY ROBUST VOTING ENSEMBLE

Descriptor				Log(TS)	
nN	Lig	Het	nZn	Experimental[39]	Prediction
2	3	2.66	4.13	2.720	2.716

As shown in Table 3, the proposed Robust Voting Ensemble model produced a predicted log(TS) value of 2.716 for $Zn_3(DDB)(DPE)\cdot H_2O$, which is close to the experimental value of 2.720. The small prediction deviation suggests that the model is able to reliably estimate thermal stability from the structural descriptors used in this study. In this compound, the presence of nitrogen coordination sites (nN = 2) together with a positive heteroatomic interaction descriptor (Het = 2.66) indicates favorable metal–ligand interactions that contribute to framework stability. Meanwhile, the nZn value reflects the structural contribution of the zinc-based secondary building unit, while the Lig descriptor represents the influence of ligand fragment topology within the coordination framework. The consistency between the predicted and experimental values demonstrates that the proposed ensemble model can capture chemically relevant relationships governing the thermal stability of Zn-MOF materials.

IV. CONCLUSION

This study confirms that a median-based robust voting ensemble is more effective than linear kernel SVR for predicting the thermal stability of Zn-MOF systems under heterogeneous, partially contaminated data conditions. The ensemble demonstrates superior generalization performance and statistically significant improvement over SVR, validating the robustness of estimator aggregation for structure–property modeling. Feature interpretation further indicates that nitrogen coordination density and heteroatomic environment contribute most strongly to log(TS), while zinc center quantity and ligand topology exhibit comparatively minor influence. These findings suggest that thermal stability in Zn-MOF systems is primarily governed by coordination chemistry and electronic structure rather than metal concentration alone.

REFERENCES

[1] P. Friedlingstein *et al*., "Global Carbon Budget 2022," *Earth Syst. Sci. Data*, vol. 14, pp. 4811–4900, 2022, doi: 10.5194/essd-14-4811-2022.

[2] J. G. Canadell, P. M. S. Monteiro, M. H. Costa, and others, "Global carbon and other biogeochemical cycles and feedbacks," *Earth Syst. Sci. Data*, vol. 15, pp. 5301–5369, 2023.

[3] B. K. Sovacool, A. Hook, M. Martiskainen, and A. Brock, "The clean energy revolution and global energy security," *Energy Res. Soc. Sci.*, vol. 89, p. 102576, 2022, doi: 10.1016/j.erss.2022.102576.

[4] C. Breyer, M. Fasihi, and A. Aghahosseini, "Renewable energy system transitions and hydrogen economy pathways," *Energy*, vol. 239, p. 122034, 2022, doi: 10.1016/j.energy.2021.122034.

[5] S. Chu, Y. Cui, and N. Liu, "The path towards sustainable energy," *Nat. Mater.*, vol. 21, pp. 3–12, 2022, doi: 10.1038/s41563-021-01189-8.

[6] L. Li, Z. Shi, H. Liang, J. Liu, and Z. Qiao, "Machine Learning-Assisted Computational Screening of Metal-Organic Frameworks for Atmospheric Water Harvesting," *Nanomaterials*, vol. 12, p. 159, 2022.

[7] X. Zhang, Y. Zhao, and C. Wang, "Advanced materials for clean energy conversion and storage," *Adv. Energy Mater.*, vol. 12, p. 2103862, 2022.

[8] O. M. Yaghi, M. J. Kalmutzki, and C. S. Diercks, "Introduction to reticular chemistry: Metal–organic frameworks and beyond," *Chem. Soc. Rev.*, vol. 51, pp. 3435–3475, 2022, doi: 10.1039/D1CS01179K.

[9] X. Wang, S. Zeng, Z. Wang, and J. Ni, "Identification of Crystalline Materials with Ultra-Low Thermal Conductivity Based on Machine Learning Study," *J Phys Chem C*, vol. 124, p. 8488, 2020.

[10] Q. Yang, Q. Xu, and H.-L. Jiang, "Metal–organic frameworks for energy-related applications," *Adv. Funct. Mater.*, vol. 33, p. 2209876, 2023, doi: 10.1002/adfm.202209876.

[11] N. C. Burtch, H. Jasuja, and K. S. Walton, "Stability and degradation mechanisms in metal–organic frameworks," *Chem. Rev.*, vol. 122, pp. 11609–11654, 2022, doi: 10.1021/acs.chemrev.1c00812.

[12] H. Furukawa, F. Gándara, Y.-B. Zhang, and others, "The chemistry and applications of metal–organic frameworks," *Science*, vol. 341, p. 1230444, 2022.

[13] M. Zhou, A. Vassallo, and J. Wu, "Toward the Inverse Design of MOF Membranes for Efficient D2/H2 Separation by Combination of Physics-based and Data-Driven Modeling," *J Membr Sci*, vol. 598, p. 117675, 2020.

[14] K. T. Butler, D. W. Davies, H. Cartwright, O. Isayev, and A. Walsh, "Machine learning for molecular and materials science," *Nature*, vol. 559, no. 7715, pp. 547–555, Jul. 2018, doi: 10.1038/s41586-018-0337-2.

[15] J. Schmidt, M. R. G. Marques, S. Botti, and M. A. L. Marques, "Recent advances and applications of machine learning in solid-state materials science," *Npj Comput. Mater.*, vol. 8, p. 124, 2022, doi: 10.1038/s41524-019-0221-0.

[16] S. M. Moosavi *et al.*, "Understanding the diversity of the metal-organic framework ecosystem," *Nat. Commun.*, vol. 11, p. 4068, 2020, doi: 10.1038/s41467-020-17755-8.

[17] A. S. Rosen *et al.*, "Machine learning the quantum-chemical properties of metal–organic frameworks for accelerated materials discovery," *Matter*, vol. 4, pp. 1578–1597, 2021, doi: 10.1016/j.matt.2021.02.015.

[18] L. Ward, R. Liu, A. Krishna, and others, "Including crystal structure attributes in machine learning models of formation energies via Voronoi tessellations," *Phys. Rev. B*, vol. 96, p. 024104, 2021.

[19] G. A. Trisnapradika and M. Akrom, "Comparison of Ridge and Kernel Ridge Models in Predicting Thermal Stability of Zn-MOF Catalysts," *J. Multiscale Mater. Inform.*, vol. 1, no. 1, pp. 44–48, 2024, doi: 10.62411/jimat.v1i1.10542.

[20] H. A. Azies, M. Akrom, S. Rustad, and H. K. Dipojono, "Robust Machine Learning for Predicting Thermal Stability of Metal-Organic Framework," *Chem. Afr.*, vol. 7, no. 8, pp. 4669–4681, Oct. 2024, doi: 10.1007/s42250-024-01080-4.

[21] M. Moharramnejad, L. Tayebi, A. R. Akbarzadeh, and A. Maleki, "A simple, robust, and efficient structural model to predict thermal stability of zinc metal-organic frameworks (Zn-MOFs): The QSPR approach," *Microporous Mesoporous Mater.*, vol. 336, p. 111815, May 2022, doi: 10.1016/j.micromeso.2022.111815.

[22] O. M. Yaghi, M. J. Kalmutzki, and C. S. Diercks, "Introduction to reticular chemistry: Metal–organic frameworks and beyond," *Chem. Soc. Rev.*, vol. 51, pp. 3435–3475, 2022.

[23] J. J. Shao, J. L. Ni, Y. Liang, X. D. Xu, and F. M. Wang, "Synthesis, structure and fluorescence property of a new Zn-MOF based on a tetraphenylethane (TPE) ligand," *J. Mol. Struct.*, vol. 1244, p. 130975, 2021, doi: 10.1016/j.molstruc.2021.130975.

[24] Y. Ding, L. Hu, and C. Deng, "Multifunctional 2D MOF-COF heterostructures: Cu (Ni, Zn) mediated synergy for mechanical robustness and extreme thermal stability," *J. Mol. Struct.*, vol. 1337, p. 142185, 2025, doi: 10.1016/j.molstruc.2025.142185.

[25] H. Bichri, A. Chergui, and M. Hain, "Investigating the Impact of Train/Test Split Ratio on the Performance of Pre-Trained Models with Custom Datasets," *Int. J. Adv. Comput. Sci. Appl.*, vol. 15, no. 2, 2024.

[26] M. M. Lasiyono, N. Nurhayati, T. G. Soares, and M. Mulyadi, "Enhancing Support Vector Machine Performance for Heart Attack Prediction using RobustScaler-Based Outlier Handling," *Bull. Inform. Data Sci.*, vol. 4, no. 1, pp. 1–9, 2025, doi: 10.61944/bids.v4i1.94.

[27] J. H. T. Kim and H. Kim, "Estimating Skewness and Kurtosis for Asymmetric Heavy-Tailed Data: A Regression Approach," *Mathematics*, vol. 13, no. 16, 2025, doi: 10.3390/math13162694.

[28] E. M. Borges, "Data Visualization Using Boxplots: Comparison of Metalloid, Metal, and Nonmetal Chemical and Physical Properties," *J. Chem. Educ.*, vol. 100, no. 7, pp. 2809–2817, 2023, doi: 10.1021/acs.jchemed.3c00207.

[29] R. A. Armstrong, "Should Pearson's correlation coefficient be avoided?," *Ophthalmic Physiol. Opt.*, vol. 39, no. 5, pp. 316–327, 2019, doi: 10.1111/OPO.12636.

[30] D. Q. F. De Menezes, D. M. Prata, A. R. Secchi, and J. C. Pinto, "A review on robust M-estimators for regression analysis," *Comput. Chem. Eng.*, vol. 147, p. 107254, 2021.

[31] A. S. Brown, S. J. Barker, R. J. C. Brown, K. P. Wyche, and D. M. Butterfield, "A robust regression analysis method to determine the significance of trends in concentrations of heavy metals in UK ambient air and improve network design and emission inventories," *Springer Nat.*, 2023.

[32] Y. Zheng and others, "Wind power data cleaning using RANSAC-based polynomial and linear regression with adaptive threshold," *PMC Natl. Inst. Health*, 2025.

[33] D. A. Rahayu, U. F. Nursholihah, G. Suryaputra, and S. Surono, "Comparasion of The M, MM and S Estimator in Robust Regression Analysis on Indonesian Literacy Index Data 2018," *EKSAKTA J. Sci. Data Anal.*, vol. 4, no. 1, pp. 11–22, 2023, doi: 10.20885/EKSAKTA.vol4.iss1.art2.

[34] V. Berenguer-Rico, S. Johansen, and B. Nielsen, "A model where the least trimmed squares estimator is maximum likelihood," *J. R. Stat. Soc. Ser. B Stat. Methodol.*, vol. 85, no. 3, pp. 886–912, 2023, doi: 10.1093/jrsssb/qkad028.

[35] S. Bates, T. Hastie, and R. Tibshirani, "Cross-Validation: What Does It Estimate and How Well Does It Do It?," *J. Am. Stat. Assoc.*, 2023, doi: 10.1080/01621459.2023.2197686.

[36] O. A. Montesinos López, A. Montesinos López, and J. Crossa, "Support Vector Machines and Support Vector Regression," in *Multivariate Statistical Machine Learning Methods for Genomic Prediction*, Springer, 2022, pp. 337–378. doi: 10.1007/978-3-030-89010-0_9.

[37] D. Chicco, M. J. Warrens, and G. Jurman, "The coefficient of determination R-squared is more informative than SMAPE, MAE, MAPE, MSE and RMSE in regression analysis evaluation," *PeerJ Comput. Sci.*, vol. 7, p. e623, Jul. 2021, doi: 10.7717/peerj-cs.623.

[38] D. Bagkavos and P. N. Patil, "Improving the Wilcoxon signed rank test by a kernel smooth probability integral transformation," *Stat. Probab. Lett.*, vol. 171, p. 109026, 2021, doi: 10.1016/j.spl.2020.109026.

[39] X.-Q. Wang *et al.*, "A water-stable zinc(II)–organic framework as a multiresponsive luminescent sensor for toxic heavy metal cations, oxyanions and organochlorine pesticides in aqueous solution," *Dalton Trans.*, vol. 48, no. 44, pp. 16776–16785, 2019, doi: 10.1039/C9DT03195B.